

1 **Online Characterization of Mixed Plastic Waste Using Machine  
2 Learning and Mid-Infrared Spectroscopy**

3  
4 Fei Long,<sup>1#</sup> Shengli Jiang,<sup>2#</sup> Adeyinka Gbenga Adekunle<sup>1</sup>, Victor M. Zavala,<sup>2</sup> Ezra Bar-Ziv<sup>1\*</sup>

5 <sup>1</sup> Department of Mechanical Engineering, Michigan Technological University, Houghton, MI,  
6 USA

7 <sup>2</sup> Department of Chemical and Biological Engineering, University of Wisconsin-Madison,  
8 Madison, WI, USA

9 \*Email: [ebarziv@mtu.edu](mailto:ebarziv@mtu.edu)

10 #Fei Long and Shengli Jiang contributed equally to this paper

11  
12 **Abstract**

13 To recycle the mixed plastic waste (MPW), it is important to obtain the compositional information  
14 online in real-time. We present a sensing platform based on a convolutional neural network (CNN)  
15 and mid-infrared spectroscopy (MIR) for the rapid and accurate characterization of MPW. The  
16 MPW samples are placed on a moving platform to mimic the industrial environment. The MIR  
17 spectra are collected at the rate of 100Hz and the proposed CNN architecture can reach an overall  
18 prediction accuracy close to 100%. Therefore, the proposed method paves the way towards the  
19 online MPW characterization in industrial applications where high throughput is needed.

20 **Synopsis Statement**

21 Combining convolutional neural network framework and mid-infrared spectroscopy for online  
22 characterization of mixed plastic waste with 100% accuracy.

23 **Keywords**

24 machine learning; mixed plastic waste; MIR spectra; classification; real-time

25

26 **1. Introduction**

27 Plastics are inexpensive and durable materials that can be easily molded into a variety of products  
28 for a wide range of applications, such as food packaging, construction, and electronics. Along with

1 the rapid growth of plastic production, the growth rate of plastic recycling is worrying. According  
2 to the U.S. Environmental Protection Agency (EPA) report in 2018<sup>[1]</sup>, 75.6% of the plastic wastes  
3 were landfilled, 15.8% were combusted, while only 8.7% were recycled. Moreover, there is a trend  
4 of decreasing recycling rate<sup>[2]</sup>, which imposes severe ecological and environmental concerns. To  
5 address the challenges, new recycling methods (pyrolysis<sup>[3]</sup>, plastic alloying<sup>[4]</sup>, etc.) are being  
6 investigated, but these solutions require an understanding of the composition of MPW in order to  
7 determine the process parameters and to remove potential contaminants<sup>[5]</sup>.

8 Non-destructive methods such as infrared (IR) spectroscopy, X-ray diffraction, laser-  
9 induced breakdown spectroscopy (LIB) and other techniques have been successfully used for the  
10 identification of a single plastic component<sup>[6-11]</sup>. Among these methods, near-infrared spectroscopy  
11 (NIR) has become the predominant technology in industry for sorting MPW. However, NIR suffers  
12 from low accuracy, partly because it cannot detect black plastics<sup>[12-13]</sup>. A promising alternative to  
13 NIR is mid-infrared spectroscopy (MIR), in which photons are transformed from the IR spectral  
14 range into the near infrared spectral range and fast silicon detectors can be used<sup>[14]</sup>. MIR  
15 spectroscopy combines the high accuracy of the infrared spectral range with the high speed of NIR.  
16 More importantly, MIR spectroscopy is capable of detecting black plastics, which can improve the  
17 accuracy of MPW characterization<sup>[15-16]</sup>.

18 In order to automate the MPW characterization process towards the industrial applications,  
19 machine learning (ML) has been widely used to analyze various spectroscopic data of plastics and  
20 the results were very promising<sup>[17-20]</sup>. However, the spectra were often the average of multiple  
21 spectroscopic scans during the data collection to reduce the intrinsic noise and to improve the ML  
22 prediction accuracy, which would slow the data collection speed. Moreover, in a typical industrial  
23 application, the MPW pellets are moved rapidly on a conveyor belt, which lowers the signal-to-

1 noise ratio (SNR) due to the vibration and disturbance of the moving platform. Therefore, a  
2 production ready MPW sorting system needs fast data collection (which we call *online*) equipment  
3 and an efficient identification algorithm to process the low SNR data.

4 In this work, we combined CNN and MIR to classify MPW on a moving platform to mimic  
5 the industrial application. The MIR spectra were collected at 100 Hz without averaging. The linear  
6 speed of the moving plastics was 0.1 m/s. We demonstrate that the CNN framework (which we  
7 call PlasticNet) can achieve 100% overall classification accuracy for MPW. The CNN framework  
8 also has a fast prediction rate (~36,000 Hz), which allows the future upgrade of the MIR  
9 spectrometer with even faster data collection speed. We believe the proposed method is a  
10 promising solution towards a real-time online MPW classification system and will help MPW  
11 recycling and reclamation.

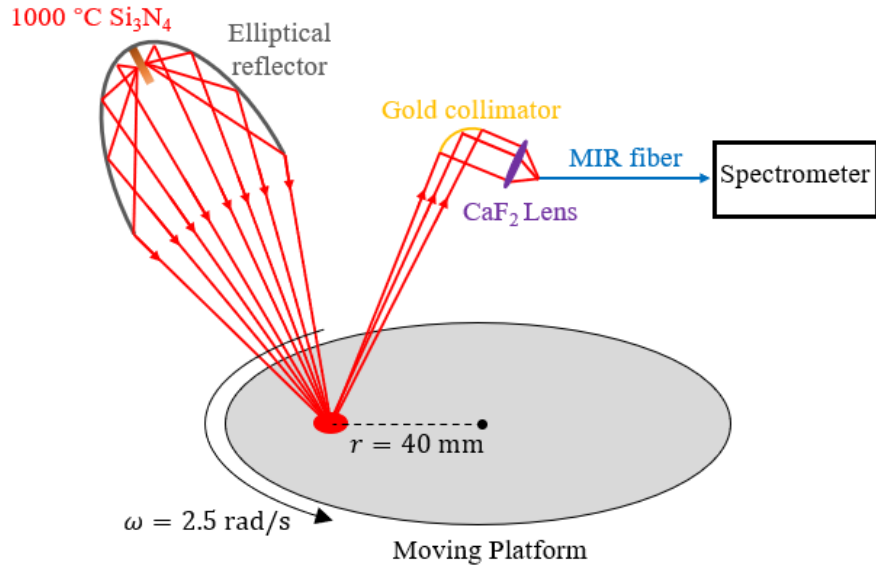
12

## 13 **2. Experimental Data Collection and Preparation**

### 14 **2.1 MIR Measuring System**

15 The schematic experimental setup is shown in **Figure 1**. The IR source (a 1000 °C Silicon  
16 Nitride,  $\text{Si}_3\text{N}_4$ , light source, 4.5 mm in diameter and 17 mm long and is heated by 70 W electric  
17 power, Hawkeye Technologies model IR-Si311) was placed at the focus of an aluminum elliptical  
18 reflector which focused the light at 200 mm from the front surface of the reflector, projecting the  
19 light on a gold diffuser, generating a circular area with around 10 mm diameter. Some of the  
20 reflected light from the plastic surface was collected by a 1-inch parabolic gold-coated aluminum  
21 mirror (with a focal length of 200 mm) that collimated light from the diffuser, after which a 40  
22 mm  $\text{CaF}_2$  lens focused the light into a 200  $\mu\text{m}$  core indium fluoride ( $\text{InF}_3$ ) fiber that was connected  
23 to the MIR spectrometer (NLIR S2050, Denmark).

1 The details of the MIR spectrometer can be found in our previous work<sup>[15]</sup>. Briefly, the  
 2 MIR spectrometer (NLIR S2050) is based on sum-frequency generation in a  $\chi(2)$ -nonlinear  
 3 LiNbO<sub>3</sub> crystal that upconverts mid-infrared light from the band 2.0  $\mu\text{m}$  – 5.0  $\mu\text{m}$  to the near-  
 4 visible region 695 nm – 877 nm<sup>[21-24]</sup>. The advantages of the upconversion spectrometer are that  
 5 most thermal noise is not upconverted<sup>[25-26]</sup> and that Silicon-based CMOS-array detectors have  
 6 much higher detectivities than the traditional MIR detectors such as HgCdTe (MCT) or PbSe array  
 7 detectors. The CMOS detector has 2048 pixels, and the spectral resolution is  $< 6 \text{ cm}^{-1}$ .



8 *Figure 1. Experimental setup. The MPW samples are placed on a moving platform to mimic  
 9 the industrial application.*

10 The MPW samples were placed on the moving platform to mimic the conveyor belt in the  
 11 industrial application. The platform was driven by a 12V DC motor. The angular velocity was set  
 12 to 2.5 rad/s and the focal point of the MIR source was 40 mm away from the center of the platform,  
 13 which corresponded to the sample linear speed of 100 m/s. The platform surface was Urethane  
 14 which was a typical conveyor belt material used in industry.

1    **2.2 Data Collection**

2    In this work we considered 4 commercially available plastic materials commonly found in the  
3    MPW, including light blue color polystyrene (PS), black color polyethylene (PE), deep blue color  
4    polypropylene (PP), and white color polyvinyl chloride (PVC). All plastic samples were 1 mm  
5    thick sheets purchased from ePlastics (San Diego, California, United States). In addition, the  
6    Urethane platform surface was also considered, and it is called the background (BK) in the  
7    following context.

8       The spectra were collected by placing the plastic samples on the moving platform. For the  
9    ML training/validation/testing, pure plastic sheets were cut to the same size as the platform, as  
10   shown in **Figure 2a**. 500 spectra of each plastic sample were collected at the measurement rate of  
11   100 Hz. Therefore, a total of 2,500 spectra were used for the ML training/validation/testing. For  
12   the ML prediction, binary and quaternary mixed plastic samples were measured as unseen data.  
13   The binary mixed plastic samples were measured by covering approximately half of the platform  
14   surface with one plastic and the other half with another plastic, as shown in **Figure 2b**. The reason  
15   of designing such binary mix was to generate the spectra dataset in which each component  
16   contributes approximately half the number of the spectra. For example, the binary mix of BK/PS  
17   dataset should have ~50% BK spectrum and ~50% of PVC spectrum. Therefore, the binary mixes  
18   can be used as the unseen data to effectively validate the accuracy of the proposed ML model. For  
19   the prediction of quaternary mixed plastic samples, the plastic sheets were cut into small flakes  
20   with sizes approximately  $20 \times 20 \text{ mm}^2$  to  $25 \times 25 \text{ mm}^2$ , then different types of plastic samples were  
21   placed on the moving platform to mimic MPW on a conveyor belt, as shown in **Figure 2c**. 4 binary  
22   combinations (BK/PS, BK/PVC, PE/PVC, PS/PP) and 1 quaternary combination (BK/PVC/PP/PS)  
23   were used, and 500 spectra of each combination were collected for the ML prediction.

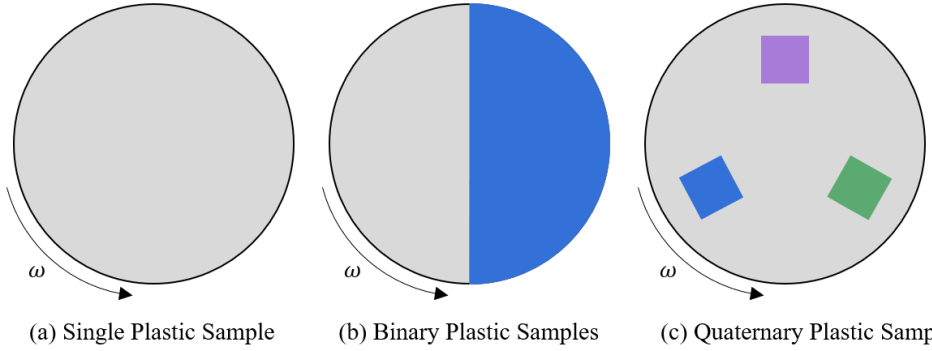


*Figure 2. Data collection methods for single, binary, and quaternary MPW samples. (a) The platform is covered by a single plastic sheet; (b) Half of the platform is covered by one plastic component, and the other half is covered by another component; (c) 3 plastic flakes are placed on the platform.*

1

## 2 2.2 Data Processing

3 Each spectrum had 975 data points ranging from wavenumber 2000 to 3500  $\text{cm}^{-1}$  (encoded in a  
 4 vector of  $\mathbb{R}^{975}$ ), with each point representing the intensity of a given wavenumber. To increase  
 5 classification accuracy, we investigated data preprocessing methods such as smoothing and  
 6 detrending. A rolling average with a window size of 30 was used for smoothing. Detrending is  
 7 accomplished by removing the linear trend (background) from the spectra. All spectra were  
 8 normalized to the range of [0, 1] to facilitate ML analysis

$$9 \quad \hat{x} = \frac{x - \min(x)}{\max(x) - \min(x)}$$

10 where  $x \in \mathbb{R}^{975}$  was the original spectrum and  $\hat{x} \in \mathbb{R}^{975}$  was the normalized spectrum. **Figure 3**  
 11 shows the PE spectra measured at 100 Hz with various preprocessing methods. The spectra of the  
 12 other 5 samples are shown in **Figure S1-4**. There was significant noise in the raw data as shown  
 13 in **Figure 3(a)** which was due to the intrinsic electronics noise at high measurement rate  
 14 (systematic noise) and the extrinsic noise due to the vibration of the moving platform. We explored  
 15 the effectiveness of various preprocessing methods on the ML prediction accuracy and provided  
 16 the best practices for preprocessing of the high noise MIR data.

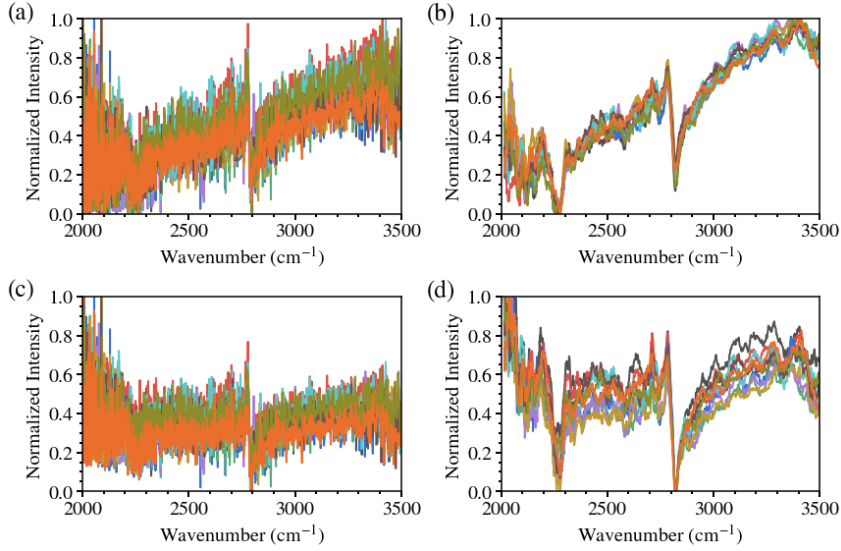


Figure 3. PE spectra measured at 100 Hz with various preprocessing methods. (a) shows the raw spectra; (b) show the smooth preprocessing; (c) shows the detrend preprocessing; (d) shows both the smooth and detrend preprocessing.

1

## 2 2.3 Data Splitting

3 The spectra of pure plastic samples as well as the Urethane platform surface (BK) were randomly  
 4 divided into a training set and a test set. A training set was used to fit the parameters of the ML  
 5 model during the learning process. An independent test set was used to evaluate the performance  
 6 (accuracy) of the ML model. A total of 30% of the spectra in the training set were randomly chosen  
 7 as the validation set for tuning the ML architecture. We employed a 5-fold cross-validation method  
 8 to assess the robustness and generalizability of the ML model. Specifically, the training dataset  
 9 was randomly split into five subsets of equal size. One of these five subsets was retained for the  
 10 cross-validation, while the other four were used for the training. The cross-validation was repeated  
 11 five times, with each subset serving as test data exactly once. Prior to data splitting, the data were  
 12 partitioned into homogeneous subsets using stratification. In other words, for each fold, each  
 13 plastic type contributed the same proportion of data (20%) to the training and test sets. The final  
 14 reported accuracy was the average of all five-fold accuracies. The model was robust and

1 generalizable if the accuracy of the test set for each fold was comparable. The spectra of the binary  
2 and quaternary plastic combinations are regarded as unseen dataset to demonstrate the MPW  
3 classification ability of the proposed ML models. For predicting the composition of mixtures, the  
4 five-fold cross validation model with the highest test set accuracy is utilized.

5 **2.4 Computational Framework**

6 The proposed framework includes a CNN architecture that we refer to as PlasticNet. PlasticNet  
7 functions as a 1D CNN since its architecture converts IR spectra to vectors (1D data items). The  
8 architecture of the proposed 1D CNN is shown in **Figure 4**. 1D CNNs extract features from IR  
9 spectra using convolution and pooling. In our architecture, every convolutional filter is a three-  
10 dimensional vector. A convolved signal of a filter is a scalar value indicating the presence (high  
11 value) or absence (low value) of the pattern the filter is attempting to identify. A convolution  
12 operation transforms a given vector to another vector of the same dimension after a nonlinear  
13 transformation (e.g., rectified linear units). These filters are referred to as the convolutional layers.  
14 The convolution operation significantly increases the amount of information that must be  
15 processed; therefore, it is necessary to summarize this information. We reduce the dimension using  
16 a max-pooling operation, which takes a subset of a given vector (in this case, a portion of size 2)  
17 and reduces it to a single value by extracting the maximum value. This greatly reduces the number  
18 of dimensions of the vector from the convolutional layer and condenses the key information.

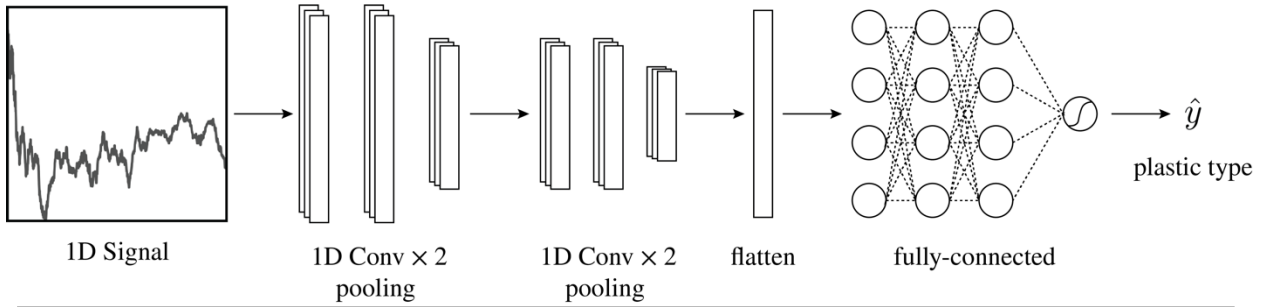


*Figure 4. Architecture of PlasticNet. The plastic network inputs a 975 vector and outputs the predicted plastic type. It contains 4 1D convolutional layers (each with 64 filters of dim 3), 2 1D max-pooling layers (each with a window size of 2), a flatten layer, and 3 fully connected layers (each with 64 nodes and a dropout ratio of 0.2). The activation function between the layers is ReLU. The final output activation function is SoftMax.*

A 975-dimensional IR vector was fed directly into the PlasticNet. Four convolutional layers, two max-pooling layers, and three fully connected layers were included in the model. Each convolutional layer contained 64 filters of size 3, whereas the max-pooling layer consists of filter of size 2. Each fully connected layer contained 64 nodes. We used rectified linear units (ReLUs) between layers as activation functions. We added a dropout ratio of 0.2 between each of two fully connected layers to prevent overfitting. The activation function of the output layer was SoftMax, and the loss function was categorical cross-entropy. The output vector had a dimension of 5, which corresponded to the probability that the IR spectra originated from a particular type of plastic.

Convolutional layers and max-pooling layers were organized recursively in the PlasticNet to extract information at both the local and global scales. In addition, it enabled the condensing of information for the classification and prediction of the corresponding plastic type.

### 3. Results and Discussion

#### 3.1 ML Training with Various Preprocessing Methods

1 The performance of the ML models with the test dataset is shown in **Table 1**. The results revealed  
2 that all preprocessing methods can achieve close to 100% classification for the single plastic  
3 component samples.

4 *Table 1. Overall Classification Accuracies Found with Different Data Processing Methods.*

	Raw	Smooth	Detrend	Both smooth and detrend
Accuracy	100%	99.8%	100%	100%

5  
6 Using the confusion matrix, we gained a deeper understanding of the classification  
7 precision of various plastic types. The PlasticNet confusion matrix of the dataset with both  
8 smoothing and detrending as preprocessing is shown in **Figure 5**. Each row of the confusion matrix  
9 represents instances of the predicted class, and each column represents instances of the true class.  
10 Instances correctly classified are in the entries along the diagonal line.

		PVC	PS	PP	PE	BK
		0.00	0.00	0.00	0.00	1.00
Predicted	PVC	0.00	0.00	0.00	1.00	0.00
	PS	0.00	0.00	0.00	1.00	0.00
	PP	0.00	0.00	1.00	0.00	0.00
	PE	0.00	1.00	0.00	0.00	0.00
	BK	1.00	0.00	0.00	0.00	0.00

11 *Figure 5. Confusion matrix of PlasticNet with both smooth and detrend preprocessing. The  
12 overall accuracy is 100%.*

13 We performed additional principal component analysis (PCA) to determine if the data  
14 possessed any inherent clustering based on the type of plastic. **Figure 6** shows the first and second

1 principal components of the MIR spectra, it is evident that clusters are formed according to plastic  
2 types. This inherent data clustering facilitated classification.

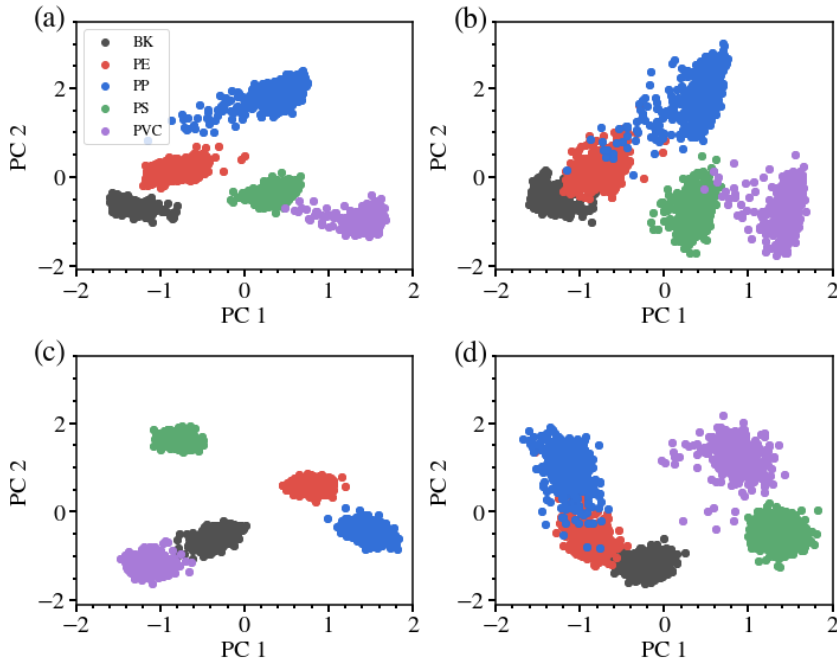


*Figure 6. Scatter plots of the first and second principal components of (a) raw IR spectra, spectra (b) after smooth preprocessing, (c) after detrend preprocessing, and (d) after both smooth and detrend preprocessing. The distinct clusters of the various plastic types facilitate classification.*

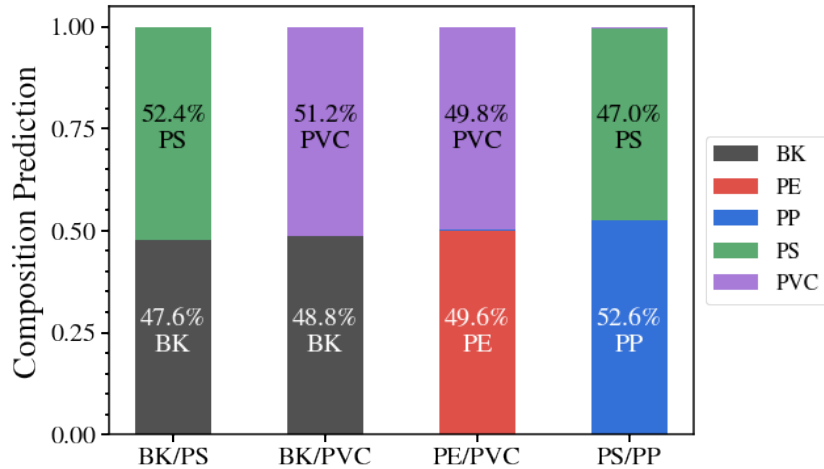
3

#### 4 **3.2 Binary Mixed Plastic Prediction**

5 We used the best of five-fold cross-validation models of various preprocessing methods to predict  
6 the composition of the binary/quaternary mixed plastics. Among all the models, the one with both  
7 smooth and detrend obtained the best results as shown in **Figure 7**. The prediction results of the  
8 models trained with other preprocessing methods (shown in **Figure S5-7**) were not accurate  
9 enough, indicating the smooth and detrend preprocessing was beneficial for ML feature extraction.

10 For the binary mixed samples BK/PS, BK/PVC, PE/PVC and PS/PP, our model predicted  
11 approximately 50% of each component. The results were consistent with our experimental design,  
12 in which the two halves of the moving platform were covered by two different plastic sheets

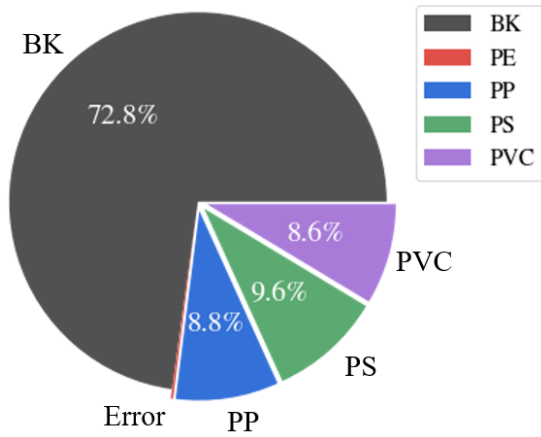
1 respectively. The percentages were not exactly 50% because during the spectra measurements, it  
2 was difficult to cover the platform surface perfectly 50%.



3 *Figure 7. Composition prediction of (a) the binary and (b) quaternary mixed plastic samples  
4 with the data using both smooth and detrend preprocessing.*

5 In addition to the correctly predicted components, we also observed prediction errors in the  
6 binary mixes, for example, 0.6% in PE/PVC and 0.4% in PS/PP. The errors were mainly from the  
7 spectra that were scanned across the boundaries of the binary mixes. In our experiments, the  
8 moving platform angular velocity was 2.5 rad/s. At 100 Hz spectra collection rate, there were 251  
9 spectra collected per revolution, in which 2 spectra were collected across the boundaries,  
10 corresponding to 0.8% boundary spectra in each binary dataset. The boundary spectra were  
11 distorted because it contained the information from both components, and depending on the level  
12 of the distortion, the ML model may make incorrect predictions. Therefore, the maximum possible  
13 error due to the boundaries should be 0.8%, and all the errors from the binary mixes were less,  
14 indicating our ML model can make correct prediction even with some of the distorted boundary  
15 spectra. Based on the results of the binary mixes, we were confident that our PlasticNet can predict  
mixed plastic samples on a moving platform with high accuracy.

1 Finally, we challenged our PlasticNet with the quaternary mix, which mimicked PVC, PP  
2 and PS flakes moving on a Urethane (BK) conveyor belt. 3 plastic flakes were placed on the  
3 moving platform, each flake was approximately  $20 \times 20 \text{ mm}^2$  to  $25 \times 25 \text{ mm}^2$ . The results are shown  
4 in **Figure 8**. The predictions were consistent with the sizes of the flakes, more importantly, there  
5 were only 0.2% of the spectra that were incorrectly classified, showing that our ML model can  
6 make accurate predictions on MPW on a moving platform.



7 *Figure 8. Composition prediction of quaternary mixed plastic samples. The prediction  
8 error is only 0.2%.*

#### 9 **4. Conclusions**

10 We developed a convolutional neural network (CNN) framework to classify the MIR spectrum  
11 of MPW on a moving platform. The experimental setup mimicked MPW on a conveyor belt. The  
12 results showed that our ML model can predict the MPW components with overall accuracy close  
13 to 100%, providing a promising solution towards the real-time online characterization of MPW for  
14 industrial applications where high throughput and accuracy are required.

#### 14 **5. Acknowledgements**

1 V.M. Zavala acknowledges funding from the U.S. National Science Foundation (NSF) under  
2 BIGDATA grant IIS-1837812. E. Bar-Ziv acknowledge funding from U.S. National Science  
3 Foundation (NSF) under PFI-RP-182736, and from the U.S. National Science Foundation (NSF)  
4 under GOALI-203366.

5

6 References:

1. EPA. Advancing Sustainable Materials Management: 2018 Fact Sheet Assessing Trends  
2 in Material Generation and Management in the United States. United States  
3 Environmental Protection Agency Research Triangle Park, Durham, NC 2020
4. A. Milbrandt, K. Coney, A. Badgett and G. T. Beckham, Quantification and evaluation of  
5 plastic waste in the United States, *Resources, Conservation and Recycling* 2022 Vol. 183  
6 Pages 106363. <https://doi.org/10.1016/j.resconrec.2022.106363>
7. Kiran, N.; Ekinci, E.; Snape, C. E. Recycling of Plastic Wastes via Pyrolysis. In  
8 *Resources, Conservation and Recycling*; 2000; Vol. 29. [https://doi.org/10.1016/S0921-3449\(00\)00052-5](https://doi.org/10.1016/S0921-3449(00)00052-5).
9. Yu, L.; Dean, K.; Li, L. Polymer Blends and Composites from Renewable Resources.  
10 *Progress in Polymer Science (Oxford)*. 2006.  
11 <https://doi.org/10.1016/j.progpolymsci.2006.03.002>.
12. da Silva, D. J.; Wiebeck, H. Current Options for Characterizing, Sorting, and Recycling  
13 Polymeric Waste. *Prog. Rubber, Plast. Recycl. Technol.* **2020**, *36* (4), 284–303.  
14 <https://doi.org/10.1177/1477760620918603>.
15. Signoret, C.; Caro-Bretelle, A. S.; Lopez-Cuesta, J. M.; Ienny, P.; Perrin, D. MIR  
16 Spectral Characterization of Plastic to Enable Discrimination in an Industrial Recycling  
17 Context: II. Specific Case of Polyolefins. *Waste Manag.* **2019**, *98*, 160–172.  
18 <https://doi.org/10.1016/j.wasman.2019.08.010>.
19. Siddiqui, M. N.; Gondal, M. A.; Redhwi, H. H. Identification of Different Type of  
20 Polymers in Plastics Waste. *J. Environ. Sci. Heal. - Part A Toxic/Hazardous Subst.*  
21 *Environ. Eng.* **2008**, *43* (11), 1303–1310. <https://doi.org/10.1080/10934520802177946>.
22. Signoret, C.; Caro-Bretelle, A. S.; Lopez-Cuesta, J. M.; Ienny, P.; Perrin, D. Alterations  
23 of Plastics Spectra in MIR and the Potential Impacts on Identification towards Recycling.  
24 *Resour. Conserv. Recycl.* **2020**, *161*, 104980.  
25 <https://doi.org/10.1016/j.resconrec.2020.104980>.
26. Wu, Q.; Yu, F.; Okabe, Y.; Saito, K.; Kobayashi, S. Acoustic Emission Detection and  
27 Position Identification of Transverse Cracks in Carbon Fiber–Reinforced Plastic  
28 Laminates by Using a Novel Optical Fiber Ultrasonic Sensing System. *Struct. Heal.*  
29 *Monit. An Int. J.* **2015**, *14* (3), 205–213. <https://doi.org/10.1177/1475921714560074>.
30. Kim, E.; Choi, W. Z. Real-time identification of plastics by types using laser-induced  
31 breakdown spectroscopy. *J. Mater. Cycles Waste Manage.* 2019, *21* (1), 176–180
32. Brunner, S.; Fomin, P.; Kargel, C. Automated sorting of polymer flakes: fluorescence  
33 labeling and development of a measurement system prototype. *Waste Manag.* 2015, *38*,  
34 49–60

12. Ragaert, K., Delva, L., Van Geem, K., 2017. Mechanical and chemical recycling of solid  
2 plastic waste. *Waste Manage.* 69, 24–58. <https://doi.org/10.1016/j.wasman.2017.07.044>

13. Faraca, Giorgia, 2019

14. Becker, W.; Sachsenheimer, K.; Klemenz, M. Detection of Black Plastics in the Middle  
5 Infrared Spectrum (MIR) Using Photon Up-Conversion Technique for Polymer  
6 Recycling Purposes. *Polymers (Basel).* **2017**, 9 (12), 435.  
7 <https://doi.org/10.3390/polym9090435>

15. Stas Zinchik, Shengli Jiang, Søren Friis, Fei Long, Lasse Høgstedt, Victor M. Zavala, and  
9 Ezra Bar-Ziv, Accurate Characterization of Mixed Plastic Waste Using Machine  
10 Learning and Fast Infrared Spectroscopy, *ACS Sustainable Chemistry & Engineering*  
11 2021 Vol. 9 Issue 42 Pages 14143-14151, DOI: 10.1021/acssuschemeng.1c04281

12. Jiang, S.; Xu, Z.; Kamran, M.; Zinchik, S.; Paheding, S.; McDonald, A.; Bar-Ziv, E.;  
13 Zavala, V. Using ATR-FTIR Spectra and Convolutional Neural Networks for  
14 Characterizing Mixed Plastic Waste. **2021**.  
15 <https://doi.org/10.26434/CHEMRXIV.14495388.V1>.

16. Development of Intelligent Sorting System Realized with the Aid of Laser-Induced  
17 Breakdown Spectroscopy and Hybrid Preprocessing Algorithm-Based Radial Basis  
18 Function Neural Networks for Recycling Black Plastic Wastes.

19. Michel, A. P. M.; Morrison, A. E.; Preston, V. L.; Marx, C. T.; Colson, B. C.; White, H.  
20 K. Rapid Identification of Marine Plastic Debris via Spectroscopic Techniques and  
21 Machine Learning Classifiers. *Environ. Sci. Technol.* 2020, 54 (17), 10630–10637.  
22 <https://doi.org/10.1021/acs.est.0c02099>.

23. Da Silva, V. H.; Murphy, F.; Amigo, J. M.; Stedmon, C.; Strand, J. Classification and  
24 Quantification of Microplastics (<100 Mm) Using a Focal Plane Array-Fourier  
25 Transform Infrared Imaging System and Machine Learning. *Anal. Chem.* 2020, 92 (20),  
26 13724–13733. <https://doi.org/10.1021/acs.analchem.0c01324>.

27. Zhu, S.; Chen, H.; Wang, M.; Guo, X.; Lei, Y.; Jin, G. Plastic Solid Waste Identification  
28 System Based on near Infrared Spectroscopy in Combination with Support Vector  
29 Machine. *Adv. Ind. Eng. Polym. Res.* 2019, 2 (2), 77–81.  
30 <https://doi.org/10.1016/j.aiepr.2019.04.001>.

31. Barh, A.; Pedersen, C.; Tidemand-Lichtenberg, P. Ultra-Broadband Mid-Wave-IR  
32 Upconversion Detection. *Opt. Lett.* **2017**, 42 (8), 1504.  
33 <https://doi.org/10.1364/ol.42.001504>.

34. Friis, S. M. M.; Høgstedt, L. Upconversion-Based Mid-Infrared Spectrometer Using  
35 Intra-Cavity LiNbO<sub>3</sub> Crystals with Chirped Poling Structure. *Opt. Lett.* **2019**, 44 (17),  
36 4231. <https://doi.org/10.1364/ol.44.004231>.

37. Jahromi, K. E.; Pan, Q.; Høgstedt, L.; Friis, S. M. M.; Khodabakhsh, A.; Moselund, P.  
38 M.; Harren, F. J. M. Mid-Infrared Supercontinuum-Based Upconversion Detection for  
39 Trace Gas Sensing. *Opt. Express* **2019**, 27 (17), 24469.  
40 <https://doi.org/10.1364/oe.27.024469>.

41. Meng, L.; Høgstedt, L.; Tidemand-Lichtenberg, P.; Pedersen, C.; Rodrigo, P. J.  
42 Enhancing the Detectivity of an Upconversion Single-Photon Detector by Spatial  
43 Filtering of Upconverted Parametric Fluorescence. *Opt. Express* **2018**, 26 (19), 24712.  
44 <https://doi.org/10.1364/oe.26.024712>.

1 25. Meng, L.; Høgstedt, L.; Tidemand-Lichtenberg, P.; Pedersen, C.; Rodrigo, P. J.  
2 Enhancing the Detectivity of an Upconversion Single-Photon Detector by Spatial  
3 Filtering of Upconverted Parametric Fluorescence. *Opt. Express* **2018**, *26* (19), 24712.  
4 <https://doi.org/10.1364/oe.26.024712>.

5 Pedersen, R. L.; Hot, D.; Li, Z. Comparison of an InSb Detector and Upconversion Detector for  
6 Infrared Polarization Spectroscopy. *Appl. Spectrosc.* **2018**, *72* (5), 793–797.  
7 <https://doi.org/10.1177/0003702817746635>.